Density Functional Theory Study of the Methylperoxy Radical Isomerization

Branko S. Jursic

Department of Chemistry, University of New Orleans, New Orleans, Louisiana 70148

Received: August 23, 1996; In Final Form: December 23, 1996[⊗]

The computational study of the high temperature $CH_3 + O_2 \rightarrow CH_3OO \rightarrow CH_2OOH \rightarrow CH_2O + OH$ radical reaction was performed. The transition state for the $CH_3OO \rightarrow CH_2OOH$ isomerization was generated using hybrid, exchange, Becke's 88, Slater's, and Xα based density functional theory (DFT) methods. A large Gaussian 6-311+G(2d,2p) type basis set was used. The computed activation barriers varied with the correlation level included in the DFT methods, as well as with the nature of the electron density approximation. The best agreement between the computed energies and geometries was obtained with the hybrid, and in some cases with the gradient-corrected, DFT methods.

Introduction

Every organic chemist who uses free radicals in research is aware that oxygen terminates the desired organic radicals by degrading the free radical−oxygen adduct. Thus, there is a significant interest in theoretically investigating the oxygen-induced degradation of free organic radicals. Due to moderate computational time and simplicity, a study of the oxygen-induced decomposition of the methyl radical was performed.

The localization of the transition state[1] on the potential energy surface is one of the most important procedures in computational chemistry.[2] From the computation of a correct reaction barrier, many fields of chemistry, as well as physics, benefit. Therefore, it is not surprising that there is a considerable interest in the computational community to have a reliable and straightforward method to elucidate transition state structures. Despite the numerous investigations in this research area, the search for transition states remains a complicated problem and a challenge for quantum mechanical methods. The accurate description of a chemical reaction requires detailed knowledge of its potential energy surface (PES). A large number of techniques are currently used to search PESs. The difficult task appears to be in locating saddle points, especially for chemical systems with a large number of degrees of freedom and an ambiguous choice of reaction coordinates.

Computational approaches based on the traditional Hartree−Fock (HF) methods contain many algorithms with different philosophies that are able to locate transition states. In many of these cases, the procedures are straightforward and relatively simple. The situation is worse in the case of DFT methods because of their convergence problem.[3] With the introduction of the energy gradient technique, as well as the use of self-consistent procedures that take into account the nonlocal corrections, the density functional theory based methods have emerged as reliable and practical tools to study the properties of large and complicated chemical systems. In addition, DFT methods require less computational effort with respect to traditional *ab initio* methods. In fact, the DFT computational time requirement increases as N^3 with the number of electrons, while the HF methods run as N^4 plus an electron correlation as N^5.

In this paper we present a computational study of the methyl peroxide radical isomerization by employing the Barny optimization algorithm for TS[4] implemented in the Gaussian computational package.[5]

Computational Methods

All of the calculations were performed using the GAUSSIAN 94 computational package.[5] Traditional Hartree−Fock (HF)[6] and second-order of a Møller−Plesset energy correction (MP2)[7] were used. Three DFT calculations were also employed: exchange functional, hybrid, and exchange functional in combination with correlation functional methods. These exchange functionals are the Slater exchange functional $\rho^{4/3}$ with a theoretical coefficient of 2/3, commonly referred to as the local spin density exchange (HFS);[8] the Xα exchange functional $\rho^{4/3}$ with an empirical coefficient of 0.7 (XALPHA);[8] and Becke's 1988 functional,[9] which includes the Slater exchange along with correlations involving the density gradient.

Three hybrid DFT methods were applied. One was Becke's three-parameter functional,[10] which has the form $AE_x^{Slater} + (1 - A)E_x^{HF} + B\Delta E_x^{Becke} + E_c^{VWN} + C\Delta E_c^{nonlocal}$, where the nonlocal correlation is provided by the LYP[11] expression (B3LYP). The constants *A*, *B*, and *C* are those determined by Becke which fit into the G1 molecular set. Becke's three-parameter functional,[10] as in B3LYP, with the nonlocal correlation provided by Perdew's 86 expression[12] (B3P86) was used. Also, Becke's three-parameter functional,[10] as in B3LYP and B3P86, but now with nonlocal correlation provided by the Perdew/Wang expression[13] (B3PW91) was used.

A combination of the exchange and correlation functional DFT methods was also employed. Three exchange functionals, Slater (S),[8] Xα (XA),[8] and Becke's 88 (B),[9] were combined with the Perdew 81 correlation functionals, (PL),[14] P86,[12] PW91,[13] LYP,[11] and the Vosko, Wilk, and Nusair 80 correlation functionals, SVWN and SVWN5.[15]

For all of the calculations, extended Gaussian type basis sets, 6-311+G(2d,2p) and 6-311++G(3df,3pd), were used. An explanation and abbreviations of the basis sets can be found in the GAUSSIAN computational package.[16]

Results and Discussion

The oxidation of the methyl radical with molecular oxygen is a complicated process that involves different competing reactions. The first step of the high-temperature CH_3 oxidation (combution) is the formation of the methylperoxy radical without an energy barrier. In a pathway that produces formaldehyde and the hydroxy radical as final products, the $CH_3OO \rightarrow CH_2$-

[⊗] Abstract published in *Advance ACS Abstracts,* February 15, 1997.

S1089-5639(96)02615-1 CCC: $14.00

TABLE 1: Geometric Parameters for the Methylperoxy Radical Generated with *ab Initio* and Density Functional Theory Methods Using the 6-311+G(2d,2p) Basis Set

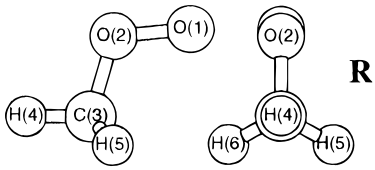

method	r21/Å	r32/Å	r43/Å	a321/deg	a432/deg	a532/deg	d4321/deg	d5321/deg
HF	1.293	1.414	1.078	111.2	105.7	109.9	180.0	60.9
MP2	1.303	1.451	1.083	110.5	105.4	111.3	180.0	60.6
B3LYP	1.318	1.449	1.087	111.3	105.4	111.2	180.0	60.6
B3P86	1.307	1.438	1.087	111.2	105.6	109.0	180.0	60.5
B3PW91	1.308	1.440	1.088	111.3	105.6	109.1	180.0	60.6
HFS	1.325	1.453	1.117	111.1	105.7	108.8	180.0	60.2
HFB	1.372	1.512	1.106	111.1	104.5	108.5	180.0	60.7
Xα	1.306	1.431	1.103	111.3	105.9	108.9	180.0	60.2
BVWN	1.348	1.477	1.087	111.3	104.9	108.7	180.0	60.6
BVWN5	1.349	1.479	1.089	111.4	104.9	108.8	180.0	60.6
BPL	1.351	1.482	1.090	111.3	104.9	108.7	180.0	60.6
BLYP	1.346	1.472	1.093	111.1	105.0	108.7	180.0	60.5
BP86	1.333	1.461	1.096	111.0	105.3	108.8	180.0	60.5
BPW91	1.331	1.460	1.094	111.1	105.3	108.9	180.0	60.5
XAVWN	1.287	1.403	1.083	111.4	106.3	109.1	180.0	60.1
XAVWN5	1.288	1.406	1.085	111.4	106.3	109.0	180.0	60.1
XAPL	1.289	1.408	1.085	111.4	106.2	109.0	180.0	60.1
XALYP	1.286	1.401	1.089	111.1	106.4	108.9	180.0	59.9
XAP86	1.276	1.393	1.092	110.9	106.7	108.8	180.0	59.8
XAPW91	1.275	1.392	1.090	111.0	106.7	108.9	180.0	59.9
SVWN	1.305	1.423	1.096	111.1	106.1	109.0	180.0	60.1
SVWN5	1.306	1.426	1.098	111.2	106.1	109.0	180.0	60.1
SPL	1.307	1.427	1.099	111.2	106.1	108.9	180.0	60.1
SLYP	1.304	1.420	1.103	110.9	106.2	108.8	180.0	60.0
SP86	1.294	1.412	1.106	110.6	106.5	108.7	180.0	59.9
SPW91	1.292	1.411	1.104	110.7	106.5	108.8	180.0	59.9

OOH isomerization occurs.[17] Because of the well-known difficulties in the theoretical characterization of radical reactions and the important role that these reactions play in the combustion process, we have selected a systematic DFT study of this radical transformation. In many of our studies we have demonstrated that some DFT methods can be used successfully for the computation of reaction barriers,[18] although there are some systems where almost all of the DFT methods fail to reproduce correct activation barriers.[19] DFT methods have a problem in the computation of activation barriers for highly exothermic reactions which have very low activation barriers (below 5 kcal/mol). The activation barriers are too low, particularly for radical reactions. We hope that on the basis of this isomerization we will be able to suggest reliable DFT methods for the investigation of similar chemical reactions.

We were not able to optimize the transition state structure for the reaction between the methyl radical and singlet oxygen. The optimization[20] produced separated reactants even when an eigenvalue-following (mode walking) optimization was used. It is well-known that with this option selected, transition state structures can be optimized under forced conditions.[21] The computation was performed by following one imaginary frequency that combined the methyl radical and singlet oxygen as reactants and the methylperoxy radical (**R**) as a product. This might be one of the instances for which DFT methods predict a "negative" activation barrier, as is the case for some other radical reactions.[19]

The geometric parameters for the methylperoxy radical (**R**) are presented in Table 1. To the best of our knowledge, the experimental data for the radical structure are not available. Considering the very high accuracy of hybrid DFT and *ab initio* MP2 methods in computing the geometries for molecular systems, we believe that these methods also produce a correct **R** structure. As in many of our previous calculations,[20] HF underestimated the bond distances, while the nonlocal methods (BVWN, BVWN5, BPL, BLYP, BP86, and BPW91) generally produced longer bond distances (Table 1). It is obvious that both the MP2 and hybrid DFT methods generated structures for **R** that are very similar to each other. On the other hand, the XA exchange functional based DFT methods (XAVWN, XAVWN5, XAPL, XALYP, XAP86, and XAPW91) considerably underestimated the bond distances, and in general, the computed values are even slightly lower than the HF computed values (Table 1). The Slater exchange functional based DFT methods (SVWN, SVWN5, SPL, SLYP, SP86, and SPW91) generated structures that are very similar to the HF *ab initio* calculations, which we know produced short bond distances.[22]

Knowing that the methylperoxy radical **R** should adopt a geometry that allows the hydrogen transfer, we have optimized the eclipsed rotamer of **R** (atoms 1−2−3−4 are in one plane) with the hope of obtaining a local minimum. This corresponds to the classical reactants complex. The optimized structures have one imaginary frequency with a rotational mode around the O(2)−C(3) bond. Thus, according to DFT methods, there is no "reactant complex" that will orient the substituent in such a way that would facilitate the proton transfer.

All of the computational methods computed transition state structures for the hydrogen transfer to the methyperoxy radical that have the position of atoms 1−2−3−4 in one plane (Table 1). Our computed structure is in very good agreement with the one computed by Saito and co-workers using MP2 *ab initio* methods.[23] The computed geometry for the transition state structure follows a similar pattern as was observed for the radical. The best agreement was obtained between the MP2 *ab initio* and hybrid DFT methods, while the nonlocal Becke's 88 correlation functional based DFT methods produced con-

TABLE 2: Geometric Parameters for the Transition State Generated with *ab Initio* and Density Functional Theory Methods Using the 6-311+G(2d,2p) Basis Set

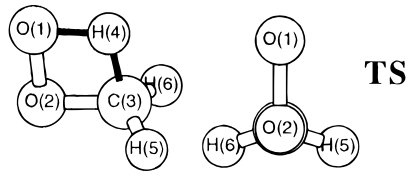

method	r21/Å	r32/Å	r41/Å	r53/Å	a321/deg	a432/deg	a532/deg	d5321/deg
HF	1.439	1.363	1.372	1.076	90.4	84.1	115.2	108.1
MP2	1.434	1.391	1.286	1.082	87.6	87.2	114.7	108.1
B3LYP	1.506	1.382	1.332	1.087	88.7	86.4	115.3	107.4
B3P86	1.484	1.377	1.322	1.087	88.7	86.3	115.3	107.4
B3PW91	1.486	1.378	1.324	1.088	88.7	86.1	115.3	107.4
HFS	1.509	1.390	1.328	1.118	88.8	88.2	115.3	107.0
HFB	1.610	1.414	1.353	1.107	87.7	87.7	115.3	107.7
Xα	1.482	1.374	1.310	1.104	88.9	88.0	115.4	107.0
BVWN	1.561	1.396	1.325	1.088	88.0	87.0	115.3	107.6
BVWN5	1.565	1.398	1.328	1.090	88.0	87.0	115.3	107.6
BL	1.566	1.399	1.329	1.091	88.0	87.1	115.3	107.6
BLYP	1.544	1.396	1.329	1.095	88.1	87.3	115.3	107.4
BP86	1.526	1.392	1.320	1.098	88.2	87.2	115.3	107.4
BPW91	1.524	1.391	1.319	1.096	88.2	87.1	115.3	107.4
XAVWN	1.450	1.356	1.283	1.086	88.8	87.9	115.4	107.0
XAVWN5	1.453	1.358	1.286	1.087	88.9	87.8	115.4	107.0
XAPL	1.454	1.359	1.286	1.088	88.9	87.8	115.4	107.0
XALYP	1.446	1.356	1.286	1.092	88.9	88.2	115.4	106.8
XAP86	1.427	1.352	1.276	1.095	88.9	88.6	115.3	106.8
XAPW91	1.427	1.351	1.275	1.093	88.9	88.4	113.4	106.7
SVWN	1.475	1.372	1.301	1.099	88.8	87.9	115.4	107.0
SVWN5	1.478	1.373	1.303	1.101	88.8	88.0	115.3	107.0
SPL	1.479	1.375	1.304	1.102	88.7	88.0	115.3	107.0
SLYP	1.471	1.372	1.304	1.106	88.8	88.3	115.3	107.8
SP86	1.450	1.368	1.293	1.109	88.8	88.7	115.2	106.8
SPW91	1.449	1.367	1.293	1.107	88.8	88.5	115.3	106.7

siderably longer bond distances (Table 2). We have determined that the reaction through this transition state structure had the highest reaction barrier in the transformation of the methyl radical and singlet oxygen into formaldehyde and the hydroxy radical.[24]

It was previously mentioned that the DFT methods exhibit considerable problems in obtaining accurate activation barriers if the values are extremely low (below 5 kcal/mol). In many of these cases, the computation of a transition state structure is impossible, or the obtained activation barrier is negative.[19] We believe that this is the reason we were not able to generate a transition state structure for the hydroxy radical elimination. In the case of the hybrid DFT computational studies, products from the radical complex were obtained (Table 3). Interestingly, all of the atoms are in one plane with an almost equidistance of O(3) from O(2) and H(1). This geometry can be expected for the electrostatic reactions at 3−1 and spin interactions at 2−3.

Computationally obtained geometries are the product of energy minimization, and it is usually harder to produce energies than geometries for chemical systems. In fact, the HF *ab initio* computational study can, in general, generate acceptable geometries for many organic molecules.[22] HF computed geometries are not acceptable in cases where polar or weak chemical bonds exist. In this case, computational methods that include an electron correlation must be used. In addition, there is a very limited number of chemical systems for which an HF computational study, even with a large basis set, can produce acceptable energies. This is a considerable problem in computing activation barriers for reactions with radicals. There are no definitive experimental results for energies of this system. It is believed that the heat of the reaction should be around −50.9 kcal/mol.[17] This is in very good agreement with the MP2 and even the HF *ab initio* computed heats. All of the DFT computational methods estimated a heat of reaction that was considerably lower than the experimental value (Table 3). Only the exchange DFT functionals (HFS, HFB, and Xα) generated energies that differ by more than 10 kcal/mol from the experimental value. The best DFT value (−48.4 kcal/mol) was computed with the B3LYP/6-311+G(2d,2p) theory model. In all of these computational studies, spin contamination is very small and negligible. For free radicals, the MP2 and DFT methods computed the S2 values to be 0.75 and 2.0 for the oxygen values, indicating no spin contamination.

The computed S2 values for the radical **R** and transition state **TS** using the HF and MP2 *ab initio* methods show a slight spin contamination, while the DFT computed S2 values, which are around 0.75, are as expected with little or no spin contamination. As for the heat of reaction, the experimental barrier for the proton transfer of the methylperoxy radical from carbon to oxygen is a subject of debate. There is no reliable information about the threshold energy for the $CH_3OO \rightarrow CH_2OOH$ transformation, since the reverse reaction has a barrier and the threshold energy is not related to the heat of reaction directly. Therefore, the calculations strongly depend on the assumption that the activation barrier is for the methylperoxy radical rearrangement. It is interesting that the barrier height for the methylperoxy radical rearrangement was assumed to be 36 kcal/mol by Reitel'bim and co-workers,[25] while Hsu and co-workers[17] estimated this barrier at 60 kcal/mol. Saito and co-workers[23] believe that the rearrangement activation barrier should be around 50 kcal/mol, with an energy threshold around 9 kcal/mol. The DFT computed reaction barrier and the threshold are presented in Table 4. The HF computed values are considerably higher than expected. MP2 with an electron correlation considerably decreases both barriers. The agreement between the computed and experimental barrier for the meth-

TABLE 3: Total Energies (au), Spin Contaminations, and Heats of Reaction (kcal/mol) for the $CH_3 + O_2 \rightarrow H_2CO + OH$ Reaction Computed Using the 6-311+G(2d,2p) Basis Set

method	E_{CH_3}	$S2_{CH_3}$	E_{O_2}	$S2_{O_2}$	E_{H_2CO}	E_{OH}	$S2_{OH}$	ΔE
HF	−39.576 250	0.761	−149.669 79	2.042	−113.907 495	−75.416 987	0.756	−49.2
MP2	−39.720 293	0.761	−150.062 72	2.050	−114.268 069	−75.597 183	0.756	−51.6
B3LYP	−39.857 489	0.753	−150.374 65	2.009	−114.545 089	−75.764 254	0.752	−48.4
B3P86	−40.016 903	0.754	−150.648 41	2.008	−114.823 173	−75.917 580	0.752	−47.3
B3PW91	−39.840 365	0.754	−150.314 26	2.009	−114.495 743	−75.732 563	0.752	−46.2
HFS	−38.911 722	0.755	−148.207 27	2.006	−112.578 815	−74.597 441	0.754	−35.9
HFB	−39.569 503	0.756	−149.802 83	2.007	−113.980 045	−75.451 833	0.753	−37.4
Xα	−39.186 103	0.756	−148.946 92	2.006	−113.211 503	−74.980 943	0.754	−37.3
BPL	−40.097 353	0.753	−150.900 51	2.005	−115.027 663	−76.045 420	0.752	−47.2
BP86	−39.849 697	0.753	−150.384 36	2.004	−114.543 603	−75.759 800	0.752	−43.5
BPW91	−39.844 794	0.754	−150.372 14	2.005	−114.531 657	−75.753 420	0.752	−42.8
BLYP	−39.826 305	0.753	−150.373 21	2.005	−114.519 505	−75.751 578	0.752	−44.9
BVWN	−40.270 265	0.753	−151.225 72	2.004	−115.345 897	−76.225 821	0.752	−47.5
BVWN5	−40.100 477	0.753	−150.910 45	2.005	−115.034 088	−76.050 663	0.752	−46.3
XAPL	−39.713 847	0.752	−150.046 34	2.004	−114.259 857	−75.574 842	0.752	−46.8
XAP86	−39.468 068	0.753	−149.531 35	2.004	−113.777 478	−75.289 453	0.752	−42.4
XAPW91	−39.463 047	0.753	−149.519 58	2.004	−113.765 749	−75.283 164	0.753	−41.6
XALYP	−39.443 922	0.753	−149.519 46	2.004	−113.752 760	−75.281 241	0.753	−44.3
XAVWN	−39.886 720	0.752	−150.371 83	2.004	−114.578 244	−75.755 288	0.752	−47.1
XAVWN5	−39.716 937	0.753	−150.056 37	2.004	−114.266 334	−75.580 087	0.752	−45.9
SPL	−39.437 636	0.752	−149.304 19	2.003	−113.624 237	−75.189 823	0.752	−45.3
SP86	−39.192 822	0.753	−148.790 07	2.003	−113.143 172	−74.905 165	0.752	−41.1
SPW91	−39.187 506	0.753	−148.777 91	2.003	−113.131 058	−74.898 620	0.752	−40.3
SLYP	−39.168 496	0.752	−148.778 24	2.004	−113.118 269	−74.895 675	0.754	−42.2
SVWN	−39.610 211	0.752	−149.629 34	2.003	−113.942 206	−75.370 053	0.752	−45.6
SVWN5	−39.440 632	0.752	−149.314 11	2.004	−113.630 596	−75.195 000	0.752	−44.5
expt[17]								−50.9

TABLE 4: Total Energies (au) and Activation Barriers (kcal/mol)[a]

method	E_R/au	S2	E_{TS}/au	S2	ΔE_I	ΔE_{II}
HF	−189.267222 1	0.763	−189.163 886 5	0.765	64.8	51.6
MP2	−189.825 133 8	0.763	−189.743 811 5	0.765	51.0	24.6
B3LYP	−190.285 750 0	0.754	−190.205 834 3	0.756	50.1	16.5
B3P86	−190.723 437 0	0.754	−190.645 472 8	0.756	48.9	12.5
B3PW91	−190.207 707 3	0.754	−190.129 211 3	0.756	49.3	15.9
HFS	−187.178 969 3	0.753	−187.111 716 0	0.755	42.2	4.6
HFB	−189.395 821	0.754	−189.320 628 4	0.755	47.2	32.4
Xα	−188.197 344 8	0.753	−188.128 281 6	0.754	43.3	3.0
BPL	−191.045 770 0	0.752	−190.968 329 3	0.755	48.6	18.5
BP86	−190.291 679 9	0.752	−190.219 218 4	0.755	45.5	9.3
BPW91	−190.270 508 7	0.752	−190.197 137 7	0.755	46.0	12.4
BLYP	−190.253 133 3	0.752	−190.178 385 0	0.755	46.9	13.3
BVWN	−191.545 210 1	0.752	−191.467 463 1	0.753	48.8	17.9
BVWN5	−191.056 918 3	0.752	−190.979 335 5	0.754	48.7	19.8
XAPL	−189.850 431 4	0.752	−189.779 671 0	0.753	44.4	−12.2
XAP86	−189.102 592 6	0.752	−189.036 935 4	0.753	41.2	−23.5
XAPW91	−189.081 695 5	0.752	−189.015 342 2	0.753	41.6	−20.5
XALYP	−189.060 905 1	0.752	−188.992 617 9	0.753	42.9	−18.3
XAVWN	−190.350 370 3	0.752	−190.279 376 8	0.753	44.5	−13.1
XAVWN5	−189.861 712 7	0.753	−189.790 827 0	0.753	44.5	−11.1
SPL	−188.827 386 8	0.752	−188.758 416 3	0.753	43.3	−10.4
SP86	−188.081 114 8	0.752	−188.017 092 6	0.753	40.2	−21.5
SPW91	−188.059 604 1	0.752	−187.994 902 4	0.753	40.6	−18.5
SLYP	−188.039 369 5	0.752	−187.972 816 1	0.753	41.8	−16.4
SVWN	−189.326 660 0	0.752	−189.257 450 0	0.753	43.4	−11.2
SVWN5	−188.838 467 7	0.752	−188.769 368 8	0.753	43.4	−9.2
expt[17]					∼50	9±5

[a] ΔE_I = total energy difference between transition state **TS** and radical intermediate **R**; ΔE_{II} = total energy difference between transition state **TS** and reactants.

ylperoxy radical isomerization is excellent. However, the reaction threshold is still too high. All of the hybrid DFT methods generated energies that are in much better agreement with the experimental results than were the MP2/6-311+G(2d,-2p) computed energies. The latter reaction threshold was ∼6 kcal/mol higher than the experimental value.

The gradient-corrected DFT methods (BPL, BP86, BPW91, BLYP, BVWN, and BVWN5), which are Becke's 88 exchange functional based DFT methods, slightly underestimated the reaction barrier. It is quite interesting that the hybrid and gradient-corrected DFT methods with the BP86 correlation functional produced threshold energies that are very close to the experimental values. On the other hand, the gradient-corrected DFT methods with the VWN and VWN5 correlation functionals tend to produce higher energies than the LYP and PW91 correlation functional based DFT methods. In many of our previous studies we have been discouraged from using the Xα and Slater's exchange functionals because the computed energies are usually much lower than the experimental values. Once again, we have demonstrated this phenomenon. The computed reaction thresholds with these two groups of DFT methods are negative, and the isomerization reaction barrier is

too low. This suggests once again that these methods should be excluded when the reaction barrier for organic free radical reactions are computed.

The isomerization barrier was previously computed by Abashkin *et al.*[24] at the MP2/MP2, MP4/MP2, QCISD(T)/MP2, and NLSD level of theory. The barriers are 51.7, 52.4, 52.6, and 49.1 kcal/mol, respectively, and they are in excellent agreement with our *ab initio* and DFT computed values (Table 4).

Preliminary computational studies of the methyl radical reaction that produces the methoxy radical and oxygen, using the hybrid DFT methods, estimated the reaction barrier to be approximately 25 kcal/mol. The computed values are in good agreement with the experimental value of 28.2 kcal/mol.[23] Thus, this suggests that the decomposition of organic radicals to the corresponding carbonyl compounds and hydroxy radical is not the most energetically preferred reaction after all.

Conclusion

The transformation of the organic radical to the peroxy radical and then to the aldehyde and hydroxy radical was studied using DFT methods. Although the transformation of an organic radical to a corresponding carbonyl compound and hydroxy radical is a difficult computational process, from these computed values it can be concluded that only the hybrid and Becke's 88 correlation functional based DFT methods are capable of describing the reaction potential energy surface. Even the energies computed with these DFT methods should be taken with caution. The heat of the reaction, isomerization reaction barrier, and the threshold energy computed using the hybrid DFT methods are 3−6 kcal/mol different from the expected experimental values. The agreement is better than the one that can be obtained using the economic HF and MP2 methods. The most reliable computational studies suggest that the carbonyl compound and hydroxy radical are probably not the product of the organic radical reaction with oxygen because of the exceptionally high reaction barrier. It is the decomposition of the methylperoxy radical to the methoxy radical and oxygen for which the hybrid DFT methods compute activation barriers to be between 30 and 40 kcal/mol.

References and Notes

(1) Kirby, A. J. *Adv. Phys. Org. Chem.* **1994**, *87*, 29. Williams, A. *Chem. Soc. Rev.* **1994**, 93. Polanyi, J. C.; Zewail, A. H. *Acc. Chem. Res.* **1995**, *28*, 119.

(2) Eksterowicz, J. E.; Houk, K. N. *Chem. Rev.* **1993**, *93*, 2439. Houk, K. N.; Li, Y.; Evanseck, J. D. *Angew. Chem. Int. Ed. Engl.* **1992**, *31*, 682. Houk, K. N.; Gonzalez, J.; Li, Y. *Acc. Chem. Res.* **1995**, *28*, 81. Fan, L.; Ziegler, T. *J. Chem. Phys.* **1990**, *92*, 3645. Fan, L.; Ziegler, T. *J. Am. Chem. Soc.* **1992**, *114*, 10890.

(3) Parr, R. G.; Yang, W. *Density Functional Theory of Atoms and Molecules*; Oxford University Press: Oxford, 1989. Dreizler, R. M.; Gross, E. K. U. *Density Functional Theory*; Springer: New York, 1990. Kryachko, E. S.; Ludeña, E. *Energy Density Functional Theory of Many-Electron Systems*; Academic: New York, 1990. *Density Functional Methods in Chemistry*, Labanowski, J., Andzelm, J., Eds.; Springer: New York, 1991. Zigler, T. *Chem. Rev.* **1991**, *91*, 651. *Modern Density Functional Theory. A Tool for Chemistry*; Seminario, J. M., Politzer, P., Eds.; Elsevier: New York, 1995.

(4) Schlegel, H. B. *J. Comput. Chem.* **1982**, *3*, 214. Gonzalez, C.; Schlegel, H. B. *J. Chem. Phys.* **1989**, *90*, 2154. Bearpark, M. J.; Robb, M. A.; Schlegel, H. B. *Chem. Phys. Lett.* **1994**, *223*, 269.

(5) Frisch, M. J.; Trucks, G. W.; Schlegel, H. B.; Gill, P. M. W.; Johnson, B. G.; Robb, M. A.; Cheeseman, J. R.; Keith, T.; Petersson, G. A.; Montgomery, J. A.; Raghavachari, K.; Al-Laham, M. A.; Zakrzewski, V. G.; Ortiz, J. V.; Foresman, J. B.; Peng, C. Y.; Ayala, P. Y.; Chen, W.; Wong, M. W.; Andres, J. L.; Replogle, E. S.; Gomperts, R.; Martin, R. L.; Fox, D. J.; Binkley, J. S.; Defrees, D. J.; Baker, J.; Stewart, J. P.; Head-Gordon, M.; Gonzalez, C.; Pople, J. A. *Gaussian 94*, Revision B.3; Gaussian, Inc.: Pittsburgh, PA, 1995.

(6) Roothan, C. C. J. *Rev. Mod. Phys.* **1951**, *23*, 69. Polple, J. A.; Nesbet, R. K. *J. Chem. Phys.* **1959**, *22*, 571. McWeeny, R.; Dierksen, G. *J. Chem. Phys.* **1968**, *49*, 4852.

(7) Møller, C.; Plesset, M. S. *Phys. Rev.* **1934**, *46*, 618. Saebo, S.; Almlof, J. *Chem. Phys. Lett.* **1989**, *154*, 83. Pople, J. A.; Binkley, J. S.; Seeger, R. *Int. J. Quant. Chem. Symp.* **1976**, *10*, 1.

(8) Slater, J. C. *Quantum Theory of Molecular and Solids.* Vol. 4: *The Self-Consistent Field for Molecular and Solids*; McGraw-Hill: New York, 1974.

(9) Becke, A. D. *Phys. Rev. A* **1988**, *38*, 3098.

(10) Becke, A. D. *J. Chem. Phys.* **1993**, *98*, 5648.

(11) Lee, C.; Yang, W.; Parr, R. G. *Phys. Rev. B* **1988**, *37*, 785. Mielich, B.; Savin, A.; Stoll, H.; Preuss, H. *Chem. Phys. Lett.* **1989**, *157*, 200.

(12) Perdew, J. P. *Phys. Rev. B* **1986**, *33*, 8822. Perdew, J. P. *Phys. Rev. B* **1987**, *34*, 7046.

(13) Perdew, J. P.; Wang, Y. *Phys. Rev. B* **1992**, *45*, 13244.

(14) Perdew, J. P.; Zunger, A. *Phys. Rev. B* **1981**, *23*, 5048.

(15) Vosko, S. H.; Wilk, L.; Nusair, M. *Can. J. Phys.* **1980**, *58*, 1200.

(16) Frisch, M. J.; Frisch, Æ.; Foresman, J. B. *Gaussian 94 User's Reference*; Gaussian, Inc.: Pittsburgh, PA, 1995.

(17) Hsu, D. S. Y.; Shaub, W. M.; Creamer, T.; Gutman, D.; Lin, M. C. *Ber. Bunsenges. Phys. Chem.* **1983**, *87*, 909.

(18) Jursic, B. S.; Zdravkovski, Z. *J. Chem. Soc., Perkin Trans. 2* **1995**, 1223. Jursic, B. S.; Zdravkovski, Z. *Int. J. Quantum Chem.* **1995**, *54*, 161. Jursic, B. S. *Chem. Phys. Lett.* **1995**, *244*, 163. Jursic, B. S. *J. Chem. Phys.* **1996**, *104*, 4151. Jursic, B. S. *J. Mol. Struct. (THEOCHEM)* **1995**, *358*, 139. Jursic, B. S. *J. Mol. Struct. (THEOCHEM)* **1995**, *244*, 263. Jursic, B. S. *J. Mol. Struct. (THEOCHEM)* **1995**, *357*, 243. Jursic, B. S. *Int. J. Quantum Chem.*, in press. Jursic, B. S. *Chem. Phys. Lett.* **1997**, *264*, 113. Jursic, B. S. *J. Mol. Chem. (THEOCHEM)* **1996**, *365*, 75.

(19) Johnson, B. G.; Gonzalez, C. A.; Gill, P. M. W.; Pople, J. A. *Chem. Phys. Lett.* **1994**, *211*, 100. Baker, J.; Andzelm, J.; Muir, M.; Taylor, P. R. *Chem. Phys. Lett.* **1995**, *237*, 53. Jursic, B. S. *Chem. Phys. Lett.* **1996**, *256*, 603. Jursic, B. S. *J. Chem. Soc., Perkin Trans. 2*, in press.

(20) DFT methods are found to be highly reliable for computing structures: Jursic, B. S.; Zdravkovski, Z. *Int. J. Quantum Chem.* **1995**, *54*, 161. Jursic, B. S. *Chem. Phys. Lett.* **1995**, *236*, 206. Jursic, B. S. *Int. J. Quantum Chem.* **1996**, *58*, 41. Jursic, B. S. *J. Mol. Struct. (THEOCHEM)* **1995**, *358*, 145. Jursic, B. S. *Int. J. Quantum Chem.* **1996**, *57*, 213. Jursic, B. S. *J. Comput. Chem.* **1996**, *17*, 835. Jursic, B. S. *Int. J. Quantum Chem.*, in press. Jursic, B. S. *J. Mol. Struct. (THEOCHEM)*, **1996**, *365*, 47.

(21) Baker, J. *J. Comput. Chem.* **1986**, *7*, 385. Baker, J. *J. Comput. Chem.* **1987**, *8*, 563.

(22) Hehre, W. J. *Practical Strategies for Electronic Structure Calculations*; Wavefunction, Inc.: Irvine, CA, 1995.

(23) Saito, K.; Ito, R.; Kakumeto, T.; Imamura, A. *J. Phys. Chem.* **1986**, *90*, 1422.

(24) Abashkin, Y.; Russo, N.; Sicilia, E.; Toscano, M. In *Modern Density Functional Theory. A Tool for Chemistry*; Seminario, J. M., Politzer, P., Eds.; Elsevier: Amsterdam, 1995; p 255.

(25) Reitel'boim, M. A.; Romanovich, L. B.; Vedeneev, B. I. *Kinet. Katal.* **1978**, *19*, 1399.

(26) Jursic, B. S. To be published.